

Satellite detection of IR precursors using bi-angular advanced along-track scanning radiometer data: a case study of Yushu earthquake

Pan Xiong · Xuhui Shen · Xingfa Gu ·
Qingyan Meng · Yaxin Bi · Liming Zhao ·
Yanhua Zhao · Yan Li · Jianting Dong

Received: 5 November 2014 / Accepted: 13 January 2015 / Published online: 10 February 2015
© The Author(s) 2015. This article is published with open access at Springerlink.com

Abstract The paper has developed and proposed a synthesis analysis method based on the robust satellite data analysis technique (RST) to detect seismic anomalies within the bi-angular advanced along-track scanning radiometer (AATSR) gridded brightness temperature (BT) data based on spatial/temporal continuity analysis. The proposed methods have been applied to analyze the Yushu (Qinghai, China) earthquake occurred on 14th April 2010, and a full AATSR data-set of 8 years data from March 2003 to May 2010 with longitude from 91°E to 101°E and latitude from 28°N to 38°N has been analyzed. Combining with the tectonic explanation of spatial and temporal continuity of the abnormal phenomena, the analyzed results indicate that the infrared radiation anomalies detected by the AATSR BT data with nadir view appear and enhance gradually along with the development and occurring of the earthquake, especially along the Ganzi-Yushu fault, Nu River fault and Jiali-Chayu fault; more infrared anomalies along the earthquake fault zone (Lancangjiang fault and

Ning Karma Monastery-Deqin fault) are detected using the proposed synthesis analysis method, which can also characterize the activity of seismic faults more precisely.

Keywords Seismic monitoring · Infrared multi-angle · Earthquake infrared radiation anomalies

1 Introduction

Satellite infrared remote sensing observation has many advantages including its large field of view, high-precision, short cycle, and not restricted by ground conditions, so it becomes the promising means to study the infrared seismic anomalies. Several studies have been carried out to analyze thermal infrared (TIR) anomalies appearing in the area of earthquake occurrence a few days before the seismic shock. These studies analytically compare images of pre (vs. post) earthquake satellite TIR imagery (Tronin et al. 2002; Shen 2013; Xie et al. 2013); study outgoing longwave radiation (OLR) data and identify anomalous variations prior to a number of medium to large earthquakes (Defu et al. 1997; Ouzounov et al. 2007; Xiong et al. 2010a, b; Jing et al. 2013; Xiong et al. 2013); perform a multispectral thermal infrared component analysis during earthquakes using land surface temperature (LST) (Ouzounov and Freund 2004; Tronin et al. 2004); or assess the anomalous surface latent heat flux (SLHF) peaks a few days prior to the earthquake event (Cervone et al. 2004, 2005; Qin 2013).

At the same time, the study of multi-angle infrared sensing mechanisms, modeling, and multi-angle remote sensing technology has made great advances, multi-angle infrared remote sensing technology and its application has promoted to develop mutually, which has become a frontier research field, but the applied research of earthquake

P. Xiong · X. Shen (✉)
Institute of Earthquake Science, China Earthquake
Administration, Beijing 100036, China
e-mail: shenxh@seis.ac.cn

X. Gu · Q. Meng · L. Zhao
Intitute of Remote Sensing Applications and Digital Earth,
Chinese Academy of Sciences, Beijing 100101, China

Y. Bi
School of Computing and Mathematics, University of Ulster,
Newtownabbey Co., Antrim BT37 0QB, UK

Y. Zhao · Y. Li · J. Dong
Beijing Institute of Space Mechanics and Electricity,
Beijing 100076, China

science using multi-angle infrared remote sensing is still blank. Therefore, the development of seismic infrared anomalies identification and extraction using multi-angle remote sensing technology, and exploring the applicability of the study of multi-angle seismic infrared radiation anomalies will be a new technology and method to study earthquake infrared remote sensing.

Actually, the main problems associated with seismic anomalies identification are lack of rigorous definition for TIR anomalies in the current study. A possible solution to these problems is to employ a new approach and an advanced data analysis technique to detect earthquake anomalies embedded in TIR remote sensing satellite data. Recently, a data analysis technique named the robust satellite data analysis technique (RST) (Tramutoli 2007) has been proposed for natural and environmental hazards monitoring and mitigation. This technique has already been validated in the case of many earthquakes (Tramutoli et al. 2001; Filizzola et al. 2004; Corrado et al. 2005; Tramutoli 2005; Aliano 2007).

Based on the characteristics of the Envisat bi-angular advanced along-track scanning radiometer (AATSR) infrared data, this paper has introduced and developed the method of the RST to detect seismic anomalies, and formed a set of data processing procedure. On this basis, this paper has carried out the case study of the Yushu earthquake occurred on 14th April 2010, combined with the tectonic explanation of the spatial and temporal continuity of the abnormal phenomena, the analyzed results have indicated a number of anomalies associated with the possible seismic characteristics of Yushu earthquake, which also has explored the applicability of multi-angle infrared remote sensing in the study of seismic infrared radiation anomalies.

2 The bi-angular AATSR data

The AATSR onboard ESA's Envisat spacecraft has three visible/near-infrared channels at 0.55, 0.67, and 0.87 micron, designed specifically for remote sensing applications over land and a visible channel at 1.6 micron which is used primarily for cloud clearing, three channels at the thermal infrared wavelengths of 3.7, 11, and 12 μm , from which surface temperatures are derived over both sea and land surfaces (Llewellyn-Jones et al. 2001). The nominal spatial resolution of AATSR is 1 km \times 1 km in the nadir view and 1.5 km \times 2 km in the forward view, with a swath width of about 500 km. Equator crossing time is 10:00 a.m. local time (descending node) and revisit time is about 3 days (Coll et al. 2012).

The AATSR has two onboard calibration mechanisms, low-noise detectors, and mechanical coolers that provide

high radiometric accuracy and stability to the TIR data (better than 0.05 K for the 11 and 12 μm bands). A special feature of the AATSR is its conical scanning mechanism to give a dual view of the Earth's surface, first in the forward view at an angle of around 55° and 150 s later in the nadir view at an angle close to vertical (from 0° to 21.7°). From two views with different atmospheric path lengths, it is possible to obtain independent information about the atmospheric contributions to the signal, and perform an accurate atmospheric correction and thus enable more precise data (ESA 2007).

The AATSR data used in this paper are usually provided in so-called Gridded Brightness Temperature/Reflectance (GBTR) product, which is the single Level 1B product from AATSR. It contains cloud-free top-of-atmosphere (TOA) brightness temperature (BT) values for the three infrared channels and reflectance values for the 1.6 μm and visible channels, and all pixels are co-located and resampled to a 1 km latitude-longitude grid (ESA 2007). In this paper, we propose to utilize the bi-angular 12- μm brightness temperature data to detect seismic anomalies using the Robust Satellite Technique.

3 Yushu earthquake

Yushu earthquake occurred on 14th April 2010, with its magnitude of 7.1, the location of the epicenter is at 33.2

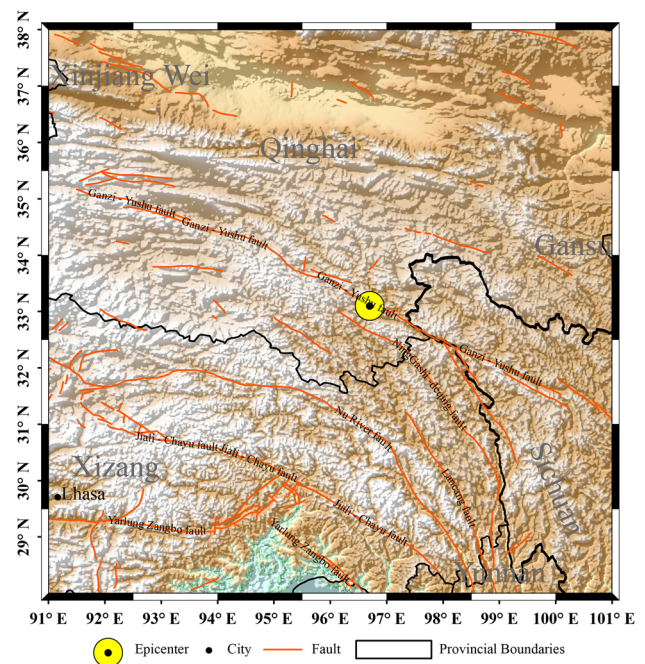


Fig. 1 The investigated area of Yushu earthquake. The epicenter of Yushu earthquake occurred on 14th April 2010 is marked with a yellow circle, the main faults are marked with pink line

north latitude, 96.6 east longitude, which is located in the Ganzi-Yushu fault zone (Fig. 1). The fault was a large strike slip fault zone of the interior of the Qinghai Tibet plateau. It was also an important boundary fault of the Sichuan-Yunnan rhombic block body (Rongjun et al. 1997). The fracture was formed in the early West HOLLEY period, and moved strongly during the Indo-Chinese epoch. Subsequently, thrust activities were the main activities of this fracture, and the fault has been a long-term active fault since the Quaternary period. The fracture was extending northwest for part of the Xianshuihe fault zone and the northern border of the Sichuan Yunnan rhombic block of Qinghai Tibet Plateau with eastward extrusion. The structure of this fault was complex (Wen et al. 1985; Wang et al. 2008; Ren et al. 2010).

4 Methodology

There are several methods to choose for the analysis of TIR data, mainly including the Eddy field calculation mean (Defu et al. 1997; Ouzounov et al. 2007), the wavelet time–frequency analysis (Cervone et al. 2005; Xiong et al. 2009a, b, 2010a, b; Xiong 2011), and the Robust Satellite data analysis Technique (Tramutoli 1998). The RST method is based on a preliminary multi-temporal analysis on several years of satellite TIR records, which is devoted to characterize the TIR signal for each pixel of the satellite image processed. This previous study concluded that IR anomalies could be identified within TIR data related to an earthquake (Tramutoli et al. 2001, 2005, 2013; Tramutoli 2005, 2007, Temimi et al. 2011). Each step of the RST method for detecting seismic anomalies using bi-angular AATSR data will be explained and detailed in the following.

4.1 Calculating the differential variable ΔT

Calculating differential variable ΔT is expected to reduce possible contributions due to day-to-day and/or year-to-year climatological changes and/or season time-drifts, the differential variable ΔT is the value of the difference between the punctual value of AATSR BT and its spatial average computed on the investigated area by taking consideration of only cloud-free locations, all belonging to the same land or sea.

The first step in calculating the differential variable ΔT is to build a cloud mask: hereinafter, we use the nadir-forward tests (Závody et al. 2000). For each pixel, the difference $T11 - T12$ is determined, and used to predict the view difference using this relationship. The actual view difference is compared with the prediction, and if they

differ by more than a pre-defined threshold, the pixel is assumed to be cloudy (ESA 2007); after performing the cloud detection, one can build an image $R_{CM}(x,y)$ for each pixel x,y of the scene $R_{CM} = 1$ or $R_{CM} = 0$ if the location has been recognized as clear or cloudy, respectively.

Given latitude and longitude of the image pixel, the surface type for each image pixel is derived from land/sea mask information obtained by an external AATSR auxiliary product; after performing the land/sea identification, one can build an image $R_{LS}(x,y)$ having for each pixel x,y of the scene with $R_{LS} = 1$ or $R_{LS} = 0$ if the location has been recognized as sea or land.

Computing the average $T(t)$ for the sea using only pixels over the scene which have $R_{CM} = 1$ and $R_{LS} = 1$ and for the land using only pixels over the scene which have $R_{CM} = 1$ and $R_{LS} = 0$.

The last step is to calculate differential variable ΔT using the formula (1)

$$\Delta T = T(r, t) - T(t), \quad (1)$$

where, $r \equiv (x, y)$ represents location coordinates of the pixel center on a satellite image; t is the time of image acquisition.

4.2 Calculating the reference field

In order to calculate the reference field for this study, we use a binning algorithm to preprocess the selected data, in which binning refers to as the process of distributing the contributions of pixels to be processed in satellite coordinates to a fixed grid using a geographic reference system. In most cases, a sinusoidal projection is used to generate a grid comprising a fixed number of equal area bins with global coverage (Campbell et al. 1995).

We use cloud-free records from the selected data-set ($t \in \tau$) to compute the reference fields for mean $\mu_{\Delta T}(r)$ and standard deviation $\sigma_{\Delta T}(r)$ at the location $r \equiv (x, y)$ using the following equations:

$$\mu_{\Delta T}(r) = \frac{1}{N} \sum_{t \in \tau}^N \Delta T(r, t) \quad (2)$$

$$\sigma_{\Delta T}(r) = \sqrt{\frac{1}{N} \sum_{t \in \tau}^N (\Delta T(r, t) - \mu_{\Delta T}(r))^2}. \quad (3)$$

A data-set used here is the bi-angular AATSR gridded BT, a coverage of longitude from 91 east longitude to 101 east longitude and latitude from 28 north latitude to 38 north latitude. The duration is from 2003 to 2010 during the months of March, April, and May has been selected and processed for computing $\mu_{\Delta T}(r)$ and $\sigma_{\Delta T}(r)$ reference fields shown in Fig. 2.

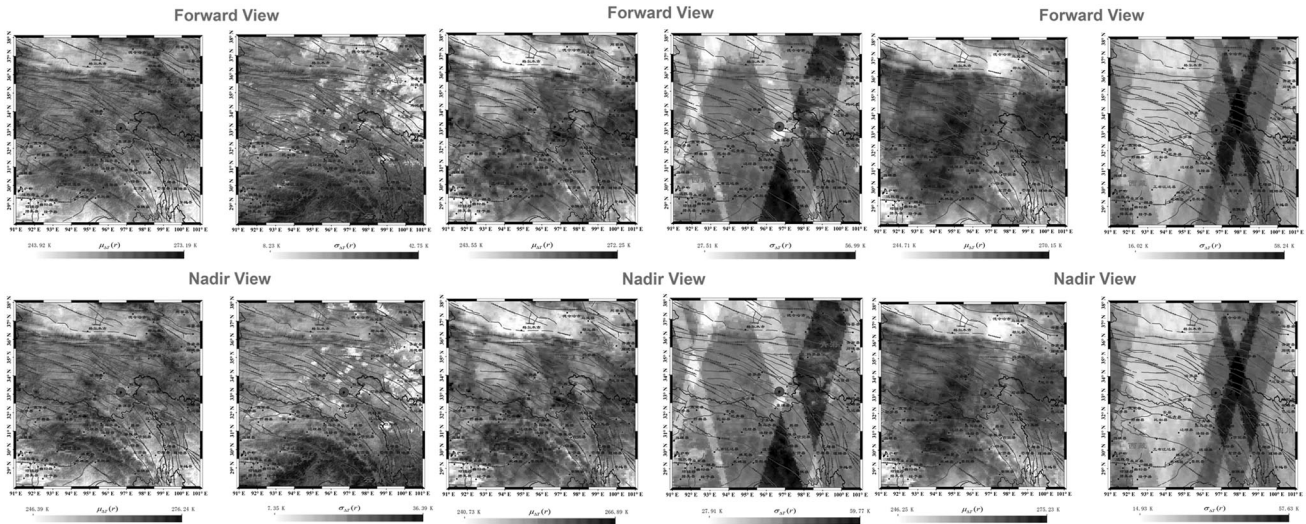


Fig. 2 The reference fields for the investigated area of forward view and nadir view computed from bi-angular AATSR data from 2003 to 2010 during the months of March (*left panel*) and April (*middle panel*) and May (*right panel*)

4.3 Anomalous detection step

Anomalous TIR of bi-angular AATSR data are detected by an index as used in (Tramutoli 2007), robust estimator of TIR anomalies (RETIRA), which can be defined as follows:

$$\otimes_{\Delta T}(r, t) = \frac{\Delta T(r, t) - \mu_{\Delta T}(r)}{\sigma_{\Delta T}(r)}. \tag{4}$$

The difference $\Delta T(r, t) - \mu_{\Delta T}(r)$ then represents the signal (S) to be investigated for its possible relation with seismic activities. It is always evaluated by comparison with the corresponding natural/observational Noise (N), represented by $\sigma_{\Delta T}(r)$ which describes the overall (local) variability of S including all (natural and observational, known, and unknown) sources of its variability, as historically observed at the same site in similar observational conditions (sensor, time of day, month, etc.). This way the relative importance of the measured TIR signal (or the intensity of anomalous TIR transients) can naturally be evaluated in terms of S/N ratio by the RETIRA index. Moreover, the larger is $\sigma_{\Delta T}(r)$, the lower will be $\otimes_{\Delta T}(r, t)$, so that the RETIRA index results intrinsically protects against false alarm proliferation (Tramutoli 2005).

4.4 The bi-angle brightness temperature synthetic approach

This paper proposes the multi-angular BT synthetic approach. In this approach, the RETIRA (Robust Estimator of TIR Anomalies) index $\otimes_{\Delta T}(r, t)$ of bi-angular AATSR BT data are processed by normalization. The Normalized Robust Estimator of TIR Anomalies index $\text{NRTIR}_{\text{nadir}}(r, t)$ can be defined as follows:

$$\text{NRTIR}_{\text{nadir}}(r, t) = \frac{\otimes_{\Delta T, \text{nadir}}(r, t) - \min(\otimes_{\Delta T, \text{nadir}}(r, t))}{\max(\otimes_{\Delta T, \text{nadir}}(r, t)) - \min(\otimes_{\Delta T, \text{nadir}}(r, t))}. \tag{5}$$

Secondly, the paper carries out the synthetic analysis of the Normalized Robust Estimator of TIR Anomalies index $\text{NRTIR}_{\text{nadir}}(r, t)$ and $\text{NRTIR}_{\text{forward}}(r, t)$ using the following equation:

$$\oplus(r, t) = 1 - (1 - \text{NRTIR}_{\text{nadir}}(r, t)) \times (1 - \text{NRTIR}_{\text{forward}}(r, t)). \tag{6}$$

Finally, the index $\oplus(r, t)$ is the multi-angular BT synthetic index within AATSR BT data, which represented the multi-angular infrared radiation characteristics.

5 Results and discussion

Using the above method and the bi-angular AATSR top-of-atmosphere BT data from 11 March, 2010 to 25 May, 2010, we get the curves of results of the RETIRA index computation on the investigated area before and after the Yushu earthquake using AATSR nadir view and forward view data. Pixels with $\otimes_{\Delta T}(r, t) > 4.0$ are depicted in mars red, pixels with $3.5 < \otimes_{\Delta T}(r, t) < 4$ are depicted in seville orange, pixels with $3.0 < \otimes_{\Delta T}(r, t) < 3.5$ are depicted in solar yellow, pixels with $2.5 < \otimes_{\Delta T}(r, t) < 3.0$ are depicted in autunite yellow, pixels with $2.0 < \otimes_{\Delta T}(r, t) < 2.5$ are depicted in yucca yellow. Epicenter is marked with red beryl green cride, the investigated area is with longitude from 91°E to 101°E and latitude from 28°N to 38°N.

5.1 Nadir view

From the results of the robust Estimator of infrared radiation Anomalies index computed on the investigated area before and after the Yushu earthquake using the AATSR BT data (Nadir view) from 11 March, 2010 to 25 May, 2010 (Fig. 3), the feature of the anomalies could be summarized as follows:

(1) About 33 days before the earthquake, on March 11th, the infrared radiation anomalies appear and enhance gradually in the course of earthquake development and occurrence along the Ganzi-Yushu fault, Nu River fault, and Jiali-Chayu fault.

(2) From March 16th to 26th, the abnormal strength rises to a maximum value, then decrease, and the infrared radiation anomalies along the Nu River fault disappear, infrared radiation anomalies on the other two faults decrease but continually develop.

On April 15th, one day after the earthquake, with the crustal stress release, the infrared radiation anomalies intensity weaken sharply along the Ganzi-Yushu fault and Jiali-Chayu fault; until the end of April, infrared radiation information becomes very weak on the two faults. On May 5th, the infrared radiation anomalies disappear along Jiali-Chayu fault. Then infrared radiation anomalies on Ganzi-Yushu fault present discrete, diffuse distribution, and disappears on May 25th at last.

In order to examine the reliability of the analyzed results for the Yushu earthquake above, this paper also carries out further analysis of infrared anomalies along faults of Yushu earthquake, this paper reduces the investigated area and selects the Ganzi-Yushu fault zone as the research area (Fig. 4).

From the results (Fig. 5) of the RETIRA index computed on the investigated area before and after the Ganzi-Yushu seismic fault using the AATSR BT data (Nadir view) from 11 March, 2010 to 25 May, 2010, we could conclude the following features: from March 11 to 31, the infrared anomalies appear in the north and south along Ganzi-Yushu fault, then gradually expand the scope, and there is an increasing trend before the earthquake; from April 5 to 15, near the earthquake time, the infrared radiation anomalies of the fault belt reach maximum, which is mainly distributed in the north and southwest side along the fault. About 7–16 days after the earthquake, many obvious anomalies still appear near the earthquake fault zone.

5.2 Forward view

From Fig. 6, we could conclude that the characteristics of infrared anomalies from forward view and Nadir view are similar, but not the same. The similar feature is that

obvious earthquake infrared radiation anomalies appear along the Ganzi-Yushu fault. However, from the results of the RETIRA index using AATSR Forward view BT data, the feature of anomalies in the area is large but the strength of anomalies decreased, the direction of the anomalies was not obvious, the process of anomalies preparation appear diffuse type, and there were not tight relationship between structure and the anomalies.

The results of the RETIRA index computed on the investigated area between nadir view (Fig. 5) and forward view (Fig. 6) data are greatly different. The possible reasons could be concluded that the local changes in development of seismic activity fault are small, but infrared anisotropy information of seismic activity is very obvious. The AATSR onboard ESA's Envisat spacecraft has a viewing geometry where each terrestrial scene is viewed at two angles, at nadir and at a forward angle of 55°. From the dual views, we get different patterns of ground, especially in complicated terrain area. And these dual views can be used to detect seismic anomalies from bi-directional observation based on infrared anisotropy of seismic activities.

5.3 Bi-angular synthetic analysis

This paper carries out the bi-angular synthetic analysis on the investigated area before and after the Yushu earthquake using the AATSR BT data (bi-angular view) from 11 March, 2010 to 25 May, 2010. From the Results (Fig. 7), the feature of the anomalies is included below:

(1) The infrared radiation anomalies appear and enhance gradually in the course of earthquake development and occurrence along the Ganzi-Yushu fault, Nu River fault and Jiali-Chayu fault, Lancang fault, and NingGashi-deqing fault from March 11th, which detect two more fault anomalies (Lancang fault and NingGashi-deqing fault) compared with the anomalies detected using the nadir view data.

(2) From March 16th to March 26th, the strength of the anomalies rises to the maximum value, then decrease. Infrared radiation anomalies along the Nu River fault reach maximum on March 21st and then disappear, infrared radiation anomalies on other several faults decrease but continually develop, and the anomalies phenomenon are obvious.

(3) On April 15th, one day after the earthquake, with the crustal strain release, infrared radiation intensity of the whole investigated area weakens sharply, and anomalies disappear on the Nanjing Temple Deqing fault. Then until the end of April, the infrared radiation feature of the earthquake on the investigated area shows discrete, diffuse distribution, no trend here.

(4) The earthquake infrared radiation on May is still present large area coverage, and the direction of seismic anomalies is not obvious, the earthquake infrared radiation anomalies disappear on May 25th.

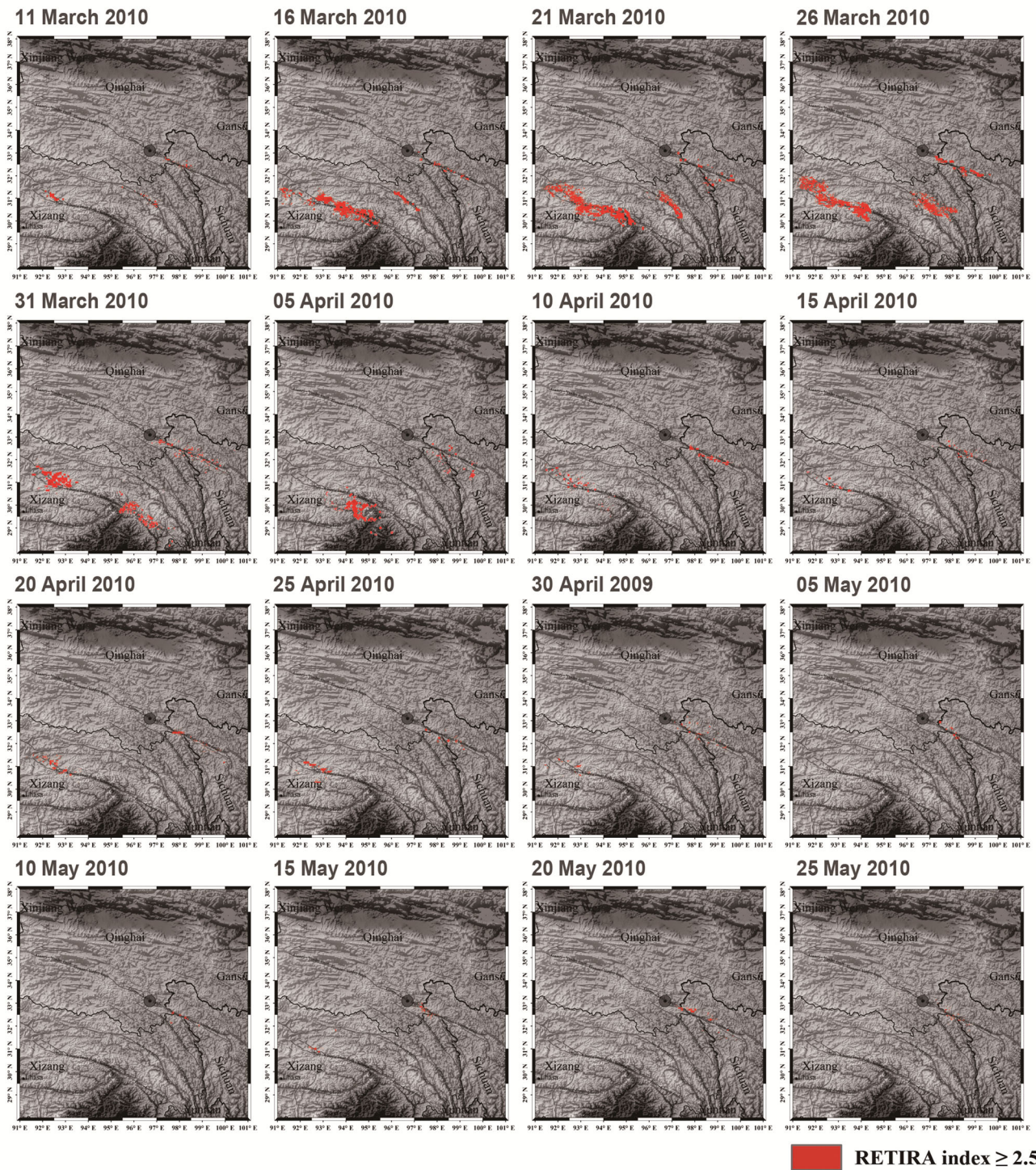


Fig. 3 Results of the RETIRA index computed on the investigated area before and after the Yushu earthquake using AATSR BT data (Nadir view)

5.4 Confutation analysis

In order to examine the reliability of the analyzed results for the Yushu earthquake above, we use the same procedure to perform a confutation analysis on a relatively

seismically unperturbed period: the same period (from 11 March to 25 May) but in a different year (2009) on the same investigated area (Fig. 8).

The anomalies from Fig. 8 are not obvious and in discontinuity. Only isolated anomalous pixels are detected.

the quick comparison between images in Fig. 3 and confutation phases (Fig. 8) allows us to realize that a substantial difference exists in the occurrence of TIR anomalies. In fact, it is evident, from the results shown in Fig. 8, that only isolated (05 April, 10 April, 15 April, 20 April, 25 April and 30 April) and not time persistent

anomalous pixels are detected. From Fig. 8, it also shows a closer view of these sporadic anomalies.

6 Conclusions

The paper has developed the methods of robust satellite data analysis techniques to detect seismic information, and formed a set of data processing procedure. On this basis, this paper has carried out the case study of Yushu (Qinghai, China) earthquake in 2010 using Envisat-AATSR bi-angular infrared data, which also has explored the applicability of multi-angle infrared remote sensing in the study of seismic infrared radiation anomalies. The main conclusions of this paper could be drawn as follows:

(1) The paper has developed the RST method to extract seismic information, which takes into account the influences of different radiation characteristics and climate, seasonal changes between cloud, land, and water, and it could eliminate the impacts on identification and extraction of seismic anomalies because of ground temperature increase effect

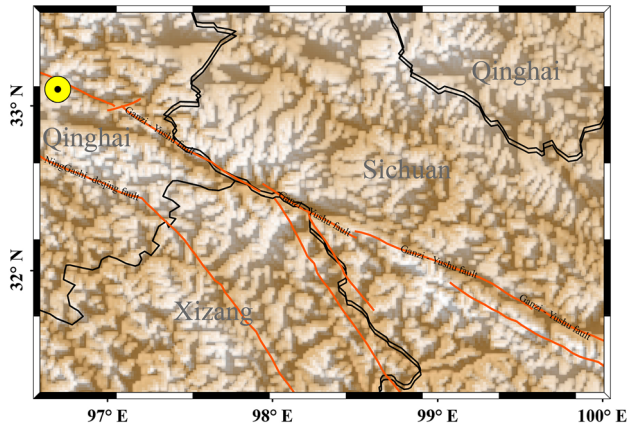


Fig. 4 The investigated area of the Ganzi-Yushu seismic fault

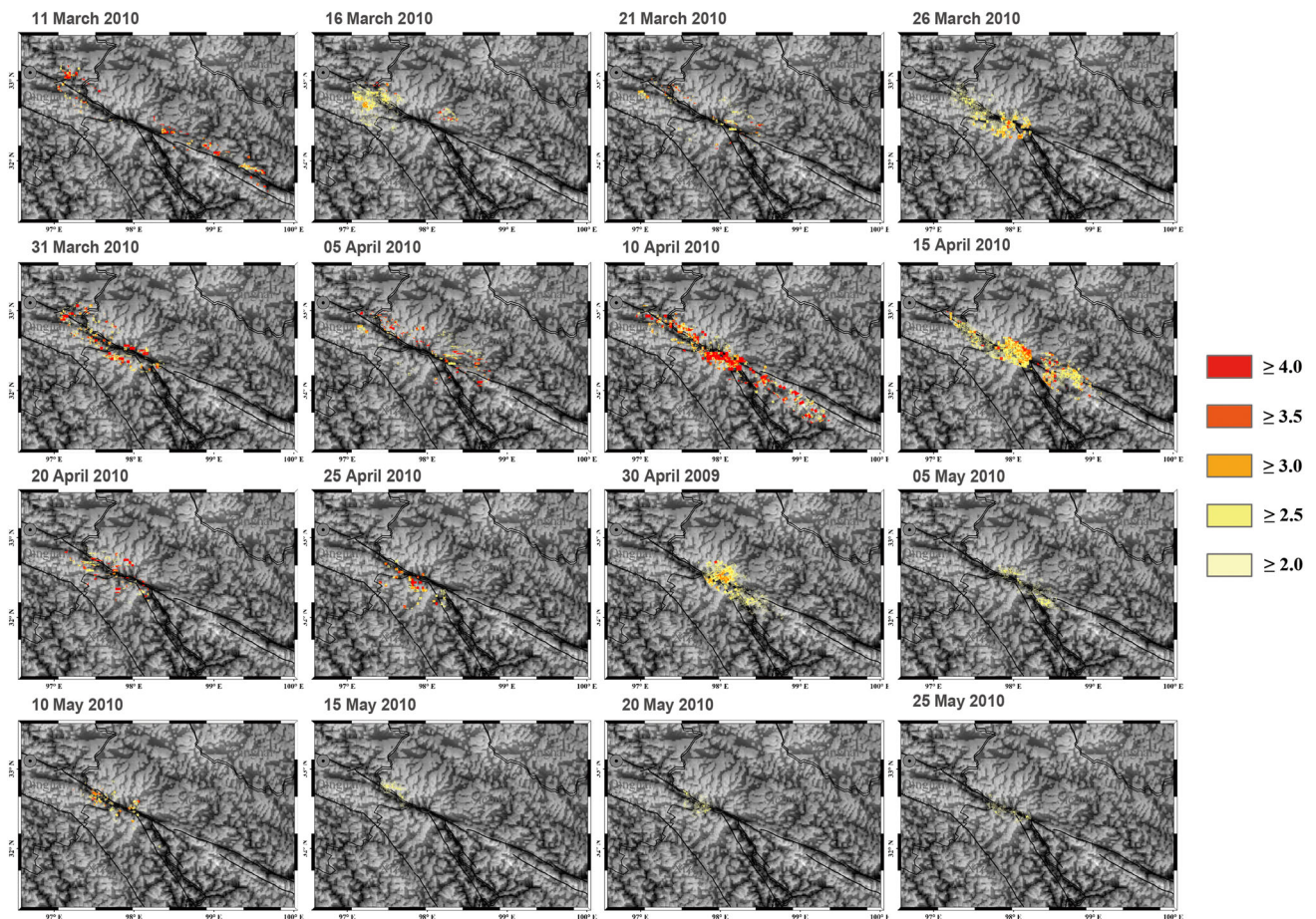


Fig. 5 Results of the RETIRA index computed on the investigated area before and after the Ganzi-Yushu seismic fault using AATSR BT data (Nadir view)

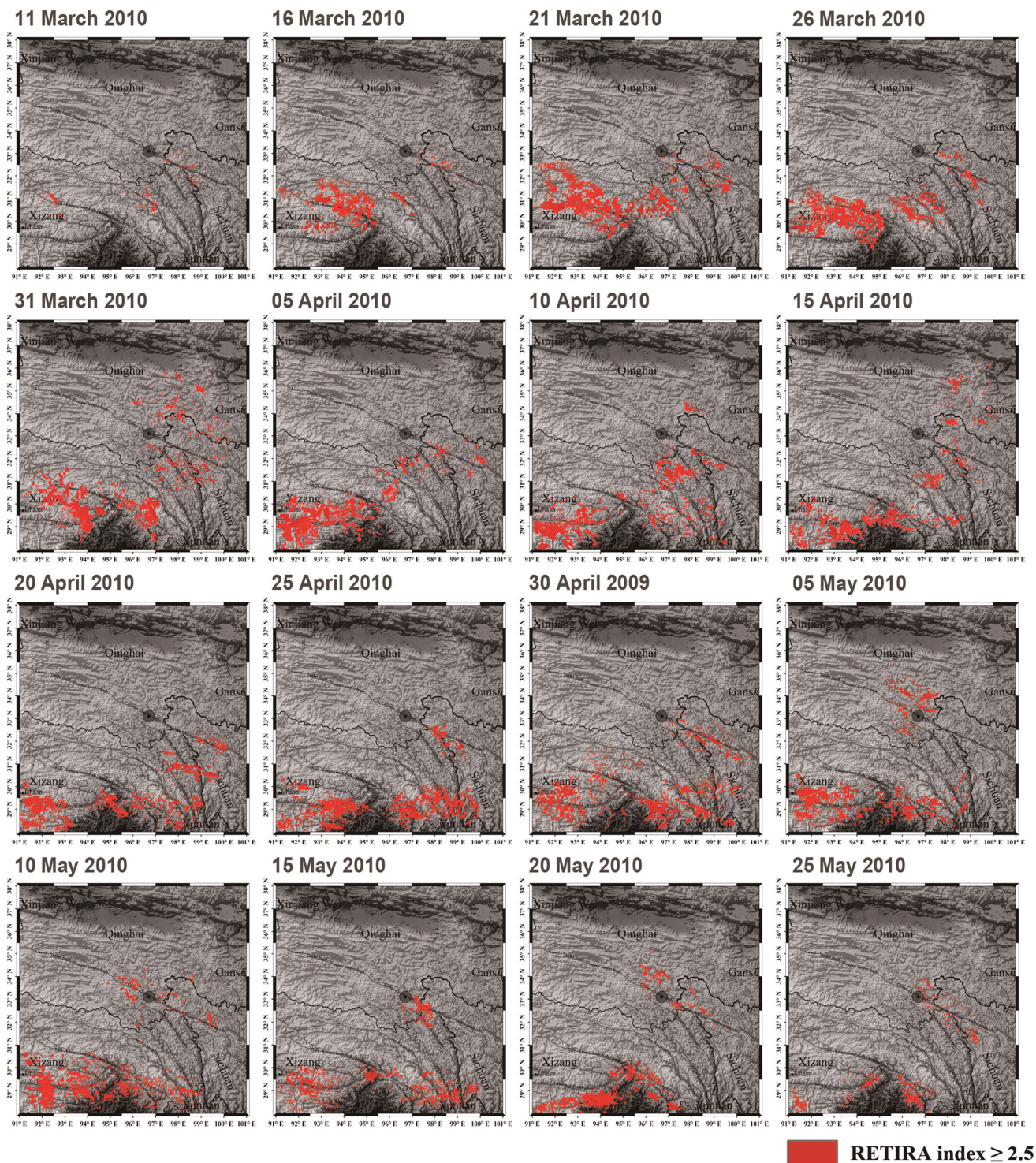


Fig. 6 Results of the RETIRA index computed on the investigated area before and after the Yushu earthquake using AATSR BT data (Forward view)

caused by seasons changing and abrupt climate variations; and based on the multi-angular background reference field for many years, the paper has used the RETIRA index to detect the seismic infrared radiation anomalies, and the detected

infrared radiation anomalies can be characterized by the signal-to-noise ratio, the greater earthquake-related noise information, and the smaller the RETIRA index, and vice versa. Therefore, the RETIRA index could avoid the infrared

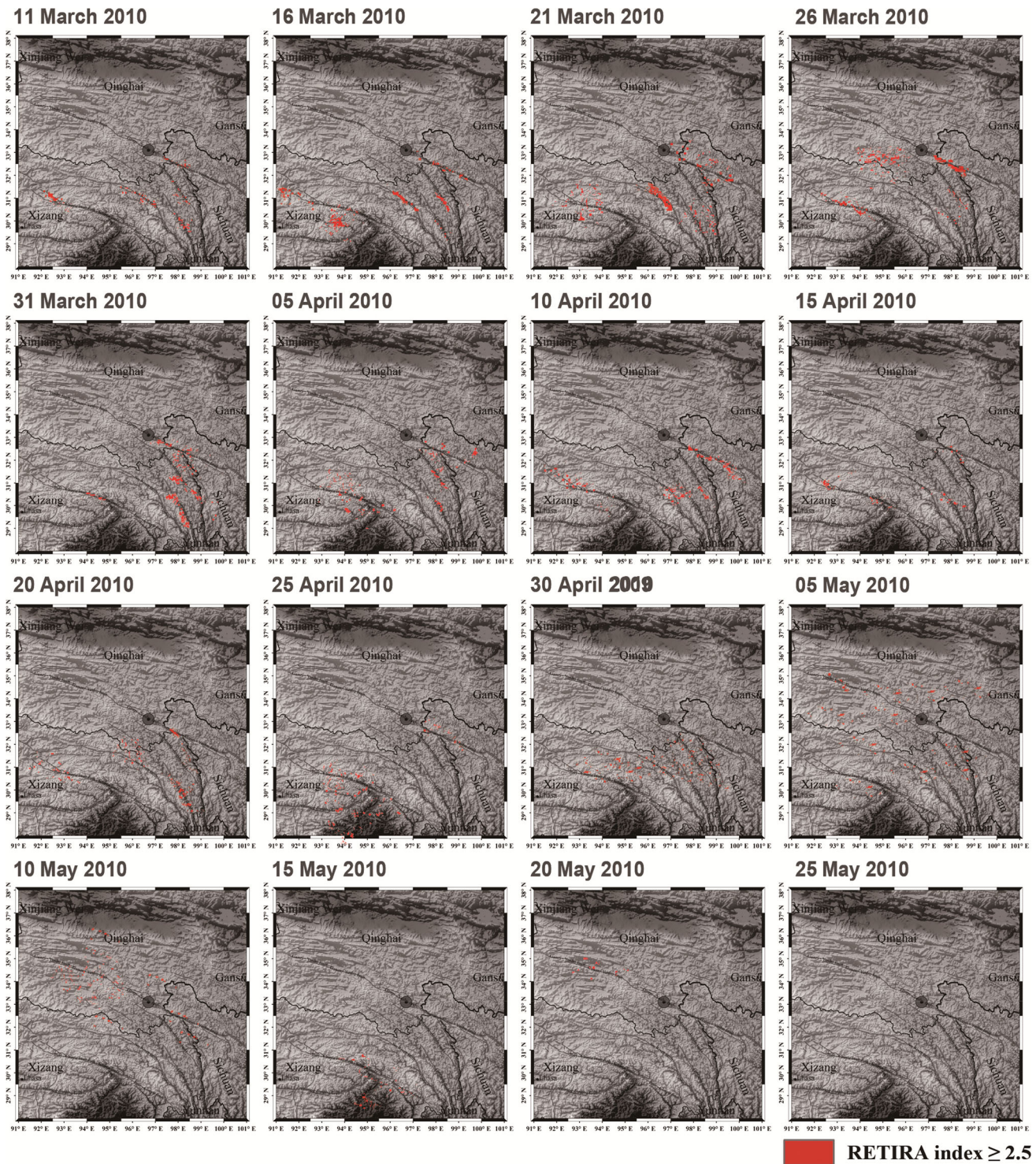


Fig. 7 Results of the RETIRA index computed on the investigated area before and after the Yushu earthquake using AATSR BT data (bi-angle synthetic analysis)

anomalies caused by non-shock, and has excellent robustness in the detected seismic infrared anomalies.

(2) The seismic anomalies characteristic detected by the AATSR nadir BT data are better than the forward BT data, which show up in that there are tighter relationships

between structure and the anomalies, the spatial and temporal development of seismic infrared radiation characteristics is more obvious, and is more close to the fault activity from the results of the RETIRA index using the nadir view data.

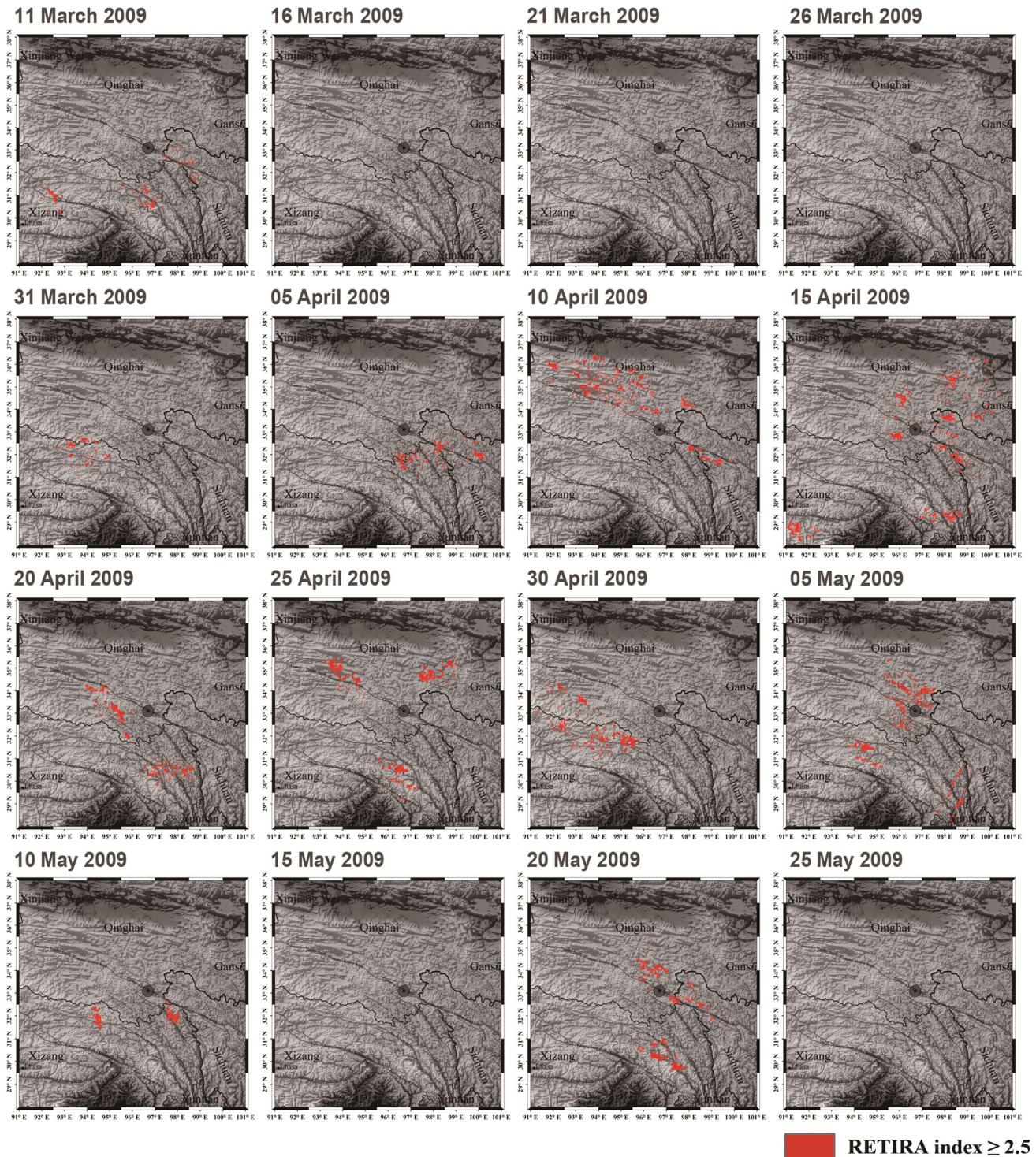


Fig. 8 Results of the RETIRA index computed on the investigated area during 2009 using AATSR BT nadir data

(3) In the case study of Yushu earthquake in 2010, the paper proposes a synthesis analysis method of the AATSR bi-angular infrared data, which efficiently analyze and synthesize the seismic infrared radiation anomalies from two different views. The result of the synthesis of seismic infrared radiation anomalies

using the AATSR nadir view and forward view data has provided more information and detected more infrared radiation anomalies along the earthquake fault zone (Lancangjiang fracture and Ning Karma Monastery-Deqin fracture), which can characterize the activity of seismic faults more precise.

Therefore our studies provide a finding that anomalies discovered within Envisat-AATSR bi-angular infrared data. This finding will be further validated using more earthquake data in the future.

Acknowledgments This work is funded by Basic Science Research Plan of Institute of Earthquake Science, China Earthquake Administration (Grant No. 2010IES0203) and Civil Specific Advance Research Program on Science, Technology, and Industry for National Defense (Grant No. 60128303). The authors would like to acknowledge European Space Agency (ESA) for making AATSR data available for various research communities, and thank referees for their useful comments.

Open Access This article is distributed under the terms of the Creative Commons Attribution License which permits any use, distribution, and reproduction in any medium, provided the original author(s) and the source are credited.

References

- Aliano C, Corrado R, Filizzola C, Pergola N, Tramutoli V (2007) Robust satellite techniques (RST) for seismically active areas monitoring: the case of 21st May, 2003 Boumerdes/Thenia (Algeria) earthquake. In: International workshop on the analysis of multi-temporal remote sensing images, 2007 (MultiTemp 2007)
- Campbell JW, Blaisdell JM, Darzi M (1995) Level-3 SeaWiFS data products: spatial and temporal binning algorithms, vol 32. NASA technical memorandum, p 104566
- Cervone G, Kafatos M, Napoletani D, Singh RP (2004) Wavelet maxima curves of surface latent heat flux associated with two recent Greek earthquakes. *Nat Hazards Earth Syst Sci* 4(3):359–374
- Cervone G, Singh RP, Kafatos M, Yu C (2005) Wavelet maxima curves of surface latent heat flux anomalies associated with Indian earthquakes. *Nat Hazards Earth Syst Sci* 5(1):87–99
- Coll C, Valor E, Galve JM, Mira M, Bisquert M, García-Santos V, Caselles E, Caselles V (2012) Long-term accuracy assessment of land surface temperatures derived from the Advanced Along-Track Scanning Radiometer. *Remote Sens Environ* 116:211–225
- Corrado R, Caputo R, Filizzola C, Pergola N, Pietrapertosa C, Tramutoli V (2005) Seismically active area monitoring by robust TIR satellite techniques: a sensitivity analysis on low magnitude earthquakes in Greece and Turkey. *Nat Hazards Earth Syst Sci* 5(1):101–108
- Defu L, Zhuoli L, Keyin P (1997) OLR anomalous phenomena before strong earthquakes. *Earthquake* 17(2):126–132
- ESA (2007) Envisat AATSR product handbook. European Space Agency, Paris
- Filizzola C, Pergola N, Pietrapertosa C, Tramutoli V (2004) Robust satellite techniques for seismically active areas monitoring: a sensitivity analysis on September 7, 1999 Athens's earthquake. *Phys Chem Earth Parts A/B/C* 29(4–9):517–527
- Jing F, Shen XH, Kang CL, Xiong P (2013) Variations of multi-parameter observations in atmosphere related to earthquake. *Nat Hazards Earth Syst Sci* 13(1):27–33
- Llewellyn-Jones D, Edwards M, Mutlow C, Birks A, Barton I, Tait H (2001) AATSR: global-change and surface-temperature measurements from Envisat. *ESA Bull* 105:11–21
- Ouzounov D, Freund F (2004) Mid-infrared emission prior to strong earthquakes analyzed by remote sensing data. *Adv Space Res* 33(3):268–273
- Ouzounov D, Liu D, Chunli K, Cervone G, Kafatos M, Taylor P (2007) Outgoing long wave radiation variability from IR satellite data prior to major earthquakes. *Tectonophysics* 431:211–220
- Qin K, Wu LX, Ouyang XY, Shen XH, Zheng S (2013) Surface latent heat flux anomalies quasi-synchronous with ionospheric disturbances before the 2007 Pu'er earthquake in China. *Adv Space Res* 1(3):2439–2454
- Ren J-J, Xie F-R, Liu D-Y, Zhang A (2010) Seismicity and recurrence Interval of Yushu 2010 earthquake, Qinghai Province. *Technol Earthq Disaster Prev* 5:228–233
- Rongjun Z, Xueze W, Changxing C, Shenghao M (1997) Recent earthquakes and assessment of seismic tendency on the Garzê-Yushu fault zone. *Seismol Geol* 19(2):115–124 (in Chinese with English abstract)
- Shen X, Zhang X, Hong S, Jing F, Zhao S (2013) Progress and development on multi-parameters remote sensing application in earthquake monitoring in China. *Earthq Sci* 26(6):427–437
- Temimi M, Lacava T, Lakhankar T, Tramutoli V, Ghedira H, Ata R, Khanbilvardi R (2011) A multi-temporal analysis of AMSR-E data for flood and discharge monitoring during the 2008 flood in Iowa. *Hydrol Process* 25(16):2623–2634
- Tramutoli V (1998) Robust AVHRR Techniques (RAT) for Environmental Monitoring theory and applications. *Earth Surf Remote Sens II* 3496:101–113
- Tramutoli V (2005) Robust satellite techniques (RST) for natural and environmental hazards monitoring and mitigation: ten years of successful applications. In: ISP MSRS 2005 conference proceedings, Beijing
- Tramutoli V (2007) Robust satellite techniques (RST) for natural and environmental hazards monitoring and mitigation: theory and applications. In: International workshop on the analysis of multi-temporal remote sensing images, 2007 (MultiTemp 2007)
- Tramutoli V, Di Bello G, Pergola N, Piscitelli S (2001) Robust satellite techniques for remote sensing of seismically active areas. *Ann Geophys* 44(2):295–312
- Tramutoli V, Cuomo V, Filizzola C, Pergola N, Pietrapertosa C (2005a) Assessing the potential of thermal infrared satellite surveys for monitoring seismically active areas: the case of Kocaeli (İzmit) earthquake, August 17, 1999. *Remote Sens Environ* 96(3–4):409–426
- Tramutoli V, Filizzola C, Pergola N (2005b) Assessing the potential of thermal infrared satellite surveys for monitoring seismically active areas: the case of Kocaeli (İzmit) earthquake, August 17 1999. *Remote Sens Environ* 96:409–426
- Tramutoli V, Aliano C, Corrado R, Filizzola C, Genzano N, Lisi M, Martinelli G, Pergola N (2013) On the possible origin of thermal infrared radiation (TIR) anomalies in earthquake-prone areas observed using robust satellite techniques (RST). *Chem Geol* 339:157–168
- Tronin AA, Hayakawa M, Molchanov OA (2002) Thermal IR satellite data application for earthquake research in Japan and China. *J Geodyn* 33(4–5):519–534
- Tronin AA, Biagi PF, Molchanov OA, Khatkevich YM, Gordeev EI (2004) Temperature variations related to earthquakes from simultaneous observation at the ground stations and by satellites in Kamchatka area. *Phys Chem Earth* 29(4–9):501–506
- Wang S, Fan C, Wang G, Wang E (2008) Late Cenozoic deformation along the northwestern continuation of the Xianshuihe fault system, Eastern Tibetan Plateau. *Geol Soc Am Bull* 120(3–4):312–327
- Wen XZ, Huang SM, Jiang ZX (1985) Neotectonic features of the Ganzi-Yushu Fault zone and assessment of its earthquake risk. *Seismol Geol* 7(3):23–32 (in Chinese with English abstract)
- Xie T, Kang CL, Ma WY (2013) Thermal infrared brightness temperature anomalies associated with the Yushu (China) *M*_s 7.1 earthquake on 14 April 2010. *Nat Hazards Earth Syst Sci* 13(4):1105–1111

- Xiong P, Bi Y, Shen X (2009a) A wavelet-based method for detecting seismic anomalies in remote sensing satellite Data. In: Perner P (ed) Machine learning and data mining in pattern recognition, vol 5632. Springer, Berlin, pp 569–581
- Xiong P, Bi YX, Shen XH (2009b) Study of outgoing longwave radiation anomalies associated with two earthquakes in China using wavelet maxima. *Hybrid Artif Intell Syst* 5572:77–87
- Xiong P, Shen X, Bi Y, Kang C, Chen L, Jing F, Chen Y (2010a) Study of outgoing longwave radiation anomalies associated with Haiti earthquake. *Nat Hazards Earth Syst Sci* 10:2169–2178
- Xiong P, Shen XH, Bi YX, Kang CL, Chen LZ, Jing F, Chen Y (2010b) Study of outgoing longwave radiation anomalies associated with Haiti earthquake. *Nat Hazards Earth Syst Sci* 10(10):2169–2178
- Xiong P, Gu X, Shen X, Zhang X, Kang C, Bi Y (2011) Wavelet-based method for detecting seismic anomalies in DEMETER satellite data. In: Xiong H, Lee WB (eds) Knowledge science, engineering and management. Springer, Berlin
- Xiong P, Gu XF, Bi YX, Shen XH, Meng QY, Zhao LM, Kang CL, Chen LZ, Jing F, Yao N, Zhao YH, Li XM, Li Y, Dong JT (2013) Detecting seismic IR anomalies in bi-angular Advanced Along-Track Scanning Radiometer data. *Nat Hazards Earth Syst Sci* 13(8):2065–2074
- Závody AM, Mutlow CT, Llewellyn-Jones DT (2000) Cloud clearing over the ocean in the processing of data from the Along-Track Scanning Radiometer (ATSR). *J Atmos Ocean Technol* 17(5):595–615